Shape and shell structure of lighter ($N \lesssim 90$) neutron-rich nuclei based on a phenomenological Woods-Saxon potential

Ikuko Hamamoto
Riken Nishina Center, Wako, Saitama 351-0198, Japan
and Division of Mathematical Physics, Lund Institute of Technology at the University of Lund, Lund S-22100, Sweden

(Received 9 October 2018; published 25 February 2019)

By using a phenomenologically successful Woods-Saxon potential, I study the shape and shell structure of (A) neutron drip line nuclei with $10 \leqslant N \leqslant 60$, (B) neutron-rich nuclei related to the r process with $40 \leqslant N \leqslant 90$, and (C) one-particle spectra in the potential provided by the nucleus ^{70}Fe as a representative of so-called $N = 40$ "island of inversion" (IoI) nuclei. First, the shell structure that is unique in very weakly bound neutrons is systematically studied, and the approximate neutron number of odd-N nuclei at which spherical (or deformed) halos can be found is pinned down. Second, the difference of the shell structure in r-process nuclei from that in stable nuclei is examined. Third, the similarity and the difference between the shell structure of $N = 20$ IoI nuclei and that of $N = 40$ IoI nuclei are analyzed. As a result, it is concluded that in Fe and Cr isotopes the deformation called "$N = 40$ IoI" continuing up to $N = 50$ is unlikely.

DOI: 10.1103/PhysRevC.99.024319

I. INTRODUCTION

In the study of nuclear many-body problems, various elaborate microscopic models starting basically with some phenomenological two-body interactions (and sometimes together with some three-body interactions) have been available. The parameters in such phenomenological models, in particular those of the two-body interactions, are usually determined so as to reproduce observed properties of nuclei around the stability line. When those models are numerically applied to nuclei far away from the stability line, it is often experienced that different models or parameters, which produce almost the same properties of stable nuclei, give quite different results of given nuclei away from the stability line. A simple well-known example is Hartree-Fock calculations using various Skyrme interactions. A model which can predict something that turns out to be in agreement with experimental data is expected to contain some essentially correct element, compared to models having various adjustable parameters so as to reproduce available data. On the other hand, microscopic models such as shell models which contain always revisable parameters are also useful for producing detailed wave functions which may be used in the analysis of data.

In the present work I try to keep the model as simple as possible when I study the shape and the shell structure of very neutron-rich nuclei away from the stability line. Then, since both shape and shell structure are essentially one-particle properties of nuclei, I work with the phenomenological one-body potential, for which the effect of neutron excess on nuclei around the stability line is in agreement with the observed data. As far as nuclear shape is concerned, the study of one-particle shell structure is definitely the first important starting point. In other words, in the present work I explore how much can be said about nuclear shape and shell structure in stable and neutron-rich nuclei using the successful phenomenological one-body potential which includes the effect of the lowest-order neutron excess, instead of starting with phenomenological two-body interactions.

I take from Ref. [1] a spherically symmetric Woods-Saxon potential in which the lowest-order effect of neutron excess, which is proportional to $(N - Z)/A$, is taken into account in the depth of the potential. Here the neutron (proton) number is expressed by N (Z), while the mass number is denoted by A. The coefficient of the $(N - Z)/A$ term was determined phenomenologically from the observed properties of neutron-rich nuclei around the stability line. One of the simple features of the Woods-Saxon potential is that the depth of the nuclear potential for neutrons (and protons) is a function of the ratio N/Z. Namely, the depth is independent of the mass A for a given N/Z. Indeed, my experience of using the Woods-Saxon potential in the study of lighter neutron-rich or neutron-halo nuclei away from the stability line has shown that the Woods-Saxon potential works remarkably well, with the result being in pretty good agreement with available experimental data. For example, see Refs. [2–4].

When deformation is suggested for certain neutron numbers by examining the shell structure for spherical shape, mainly due to the approximate degeneracy of one-particle eigenenergies of spherically symmetric potentials (Jahn-Teller effect), the shell structure in the axially symmetric quadrupole-deformed potential is further studied for those neutron numbers. The successful example of finding the region of nuclei with possible quadrupole deformation in the present way is the deformed stable rare-earth nuclei [5]. Namely, for some proton numbers which accept prolate deformation, nuclei with $90 \leqslant N \leqslant 112$ are deformed. For those neutron numbers the energies of most one-particle levels occupied in the last major shell decrease (downward-going

levels) for the relevant deformation parameter $\beta > 0$. See, for example, Fig. 5-3 in Ref. [5]. This means that a very rough estimate of the total energy, which is just the sum of one-particle energies of occupied orbits, decreases for the relevant range of prolate deformation of those nuclei compared with spherical shape. This rare-earth example describes the deformed nuclei within one major shell, $82 \leqslant N \leqslant 126$, where the pair correlation is important. Due to the presence of pair correlation, deformed shape is not obtained immediately after neutrons start to occupy the major shell. The same idea was applied to lighter nuclei, neutron-rich Mg isotopes with a smaller degeneracy (only the $1f_{7/2}$ and $2p_{3/2}$ shells), and the deformation of Mg isotopes with $N = 21$–26 [2] was successfully predicted. Noting that the observed absolute dominance of prolate deformation over oblate deformation in the ground state of even-even deformed nuclei is not yet really understood [6], in the present work I do not consider the possibility of oblate shape for the ground state of even-even nuclei.

One-particle energy spectra in the quadrupole-deformed potential are known to have a close relation to the observed low-lying energy spectra in odd-A deformed nuclei [5]. In other words, the one-particle picture in deformed nuclei seems to work much better than that in spherical nuclei. Namely, in nuclei with spherical shape one-particle energies may be compared with low-lying spectra at best only in the (spherical closed-shell plus/minus one nucleon) nuclei. In contrast, in deformed nuclei it is known that the one-particle picture works well in most odd-A well-deformed stable rare-earth nuclei [5]. This is certainly because in the phenomenological quadrupole-deformed potential the major part of the residual interaction in the spherical potential, quadrupole-quadrupole interaction, is already included in the one-body potential.

In the present article first I show the neutron shell structure in the spherically symmetric potential unique in neutron drip line nuclei with $10 < N < 60$ by taking $N/Z = 2$. The observed heaviest odd-N nuclei for given even Z are, for example, ${}^{19}_{6}C_{13}$, ${}^{23}_{8}O_{15}$, ${}^{31}_{10}Ne_{21}$, ${}^{37}_{12}Mg_{25}$, and so on. Therefore, the ratio $N/Z = 2$ is an approximate estimate of the even-even core for odd-N nuclei with the last bound odd neutron. The ratio may, of course, change in heavier isotopes. Second, I am interested in the neutron shell structure of a spherically symmetric potential in nuclei around the r process. Here the Fermi level may be expected around -3 to -5 MeV, which corresponds to the ratio $N/Z \approx 1.7$ in the lighter mass region of the r process. Since actual nuclei involved in the r process have a finite temperature, the information on the shell structure of particle spectra may not be directly obtained from observation. Nevertheless, the information on the shape and shell structure in the considered neutron-rich nuclei is basically important for understanding the structure of the r process. The shell structure of the neutron spectra obtained will be compared with that of stable nuclei in the region of the same neutron number. Third, as an example of going one step further from the shell structure related to the spherically symmetric potential, taking the shell structure obtained for a quadrupole deformed potential I study the nuclei ${}^{70}_{26}Fe_{44}$ and ${}^{66}_{24}Cr_{42}$, for which the ratio is $N/Z \approx 1.7$, though those nuclei are a bit too light to have something to do with the r process. Those nuclei were recently studied intensively both experimentally [7–9] and theoretically and have a typical shell structure which indicates the possibility of having deformed shape similar to the shell structure of nuclei with $N \approx 20$, called the "island of inversion" (IoI). My intention is to look for a general basic sign of deformation appearing already in one-particle spectra of the spherical one-body potential before going to complicated microscopic calculations which necessarily contain various parameters.

In Sec. II the main points of the model used are briefly summarized, while the results of numerical calculations are given in Sec. III. In Sec. III A the shell structure unique to the neutron drip line is exhibited for $10 < N < 60$, while in Sec. III B the shell structure in neutron-rich nuclei with $40 < N < 90$ expected in the region of lighter nuclei around the r process is shown and discussed in comparison with that in stable nuclei. In Sec. III C nuclei ${}^{70}_{26}Fe_{44}$ and ${}^{66}_{24}Cr_{42}$, which belong to the part of the lightest mass region in Sec. III B, namely the region of "IoI around N=40," are chosen to discuss the possible spherical or deformed shape based on the shell structure. The conclusion and discussions are given in Sec. IV.

II. MODEL

As a one-body nuclear potential I take the Woods-Saxon potential described in pp. 238–240 of Ref. [1], for which the neutron-excess term determined phenomenologically by the properties of stable nuclei has worked pretty well in the analysis of light neutron drip line nuclei. For example, see Refs. [2,3]. In order to systematically study the shape and shell structure of neutron-rich nuclei away from the stability line, in the present work I choose to start not with a two-body interaction but directly with the one-body potential, for which the parameters are phenomenologically determined. When observed properties of the ground state of nuclei indicate that nuclei are not spherical, the relevant deformation is almost always axially symmetric quadrupole deformation. Therefore, as deformation in the present article I consider only axially symmetric quadrupole deformation. Though the Hamiltonian and the related formula are the same as those given in Ref. [10], for completeness I give a brief summary of them in the following. The axially symmetric quadrupole-deformed potential for neutrons consists of the following three parts:

$$V(r) = V_{WS}\, f(r), \tag{1}$$

$$V_{\rm coupl}(\vec{r}) = -\beta k(r) Y_{20}(\hat{r}), \tag{2}$$

$$V_{so}(r) = -V_{WS}\, v \left(\frac{\Lambda}{2}\right)^2 \frac{1}{r}\frac{df(r)}{dr}\,(\vec{\sigma}\cdot\vec{\ell}), \tag{3}$$

where Λ is the reduced Compton wave-length of nucleon $\hbar/m_r c$,

$$f(r) = \frac{1}{1+\exp\left(\frac{r-R}{a}\right)}, \tag{4}$$

and

$$k(r) = RV_{WS}\frac{df(r)}{dr}. \tag{5}$$

Though the expression of the spin-orbit potential (3) is slightly different from the one in Ref. [1], the value of $v = 32$ which I use produces the same spin-orbit potential given in Ref. [1]. When the shell structure of protons is studied, the Coulomb potential for protons is included in the one-body potential. The values of parameters in the one-body potentials are taken from Ref. [1]. The point related to the present work is that the parameters in the potential connected to neutron excess are taken from the properties of the stable neutron-rich nuclei.

I write the single-particle wave-function in the body-fixed (intrinsic) coordinate system as

$$\Psi_\Omega(\vec{r}) = \frac{1}{r}\sum_{\ell j} R_{\ell j\Omega}(r)\,\mathbf{Y}_{\ell j\Omega}(\hat{r}), \tag{6}$$

which satisfies

$$H\,\Psi_\Omega = \varepsilon_\Omega\,\Psi_\Omega, \tag{7}$$

where Ω expresses the component of one-particle angular momentum along the symmetry axis and is a good quantum number. The coupled differential equations for the radial wave functions are written as

$$\left(\frac{d^2}{dr^2} - \frac{\ell(\ell+1)}{r^2} + \frac{2m}{\hbar^2}[\varepsilon_\Omega - V(r) - V_{so}(r)]\right)R_{\ell j\Omega}(r)$$
$$= \frac{2m}{\hbar^2}\sum_{\ell' j'}\langle \mathbf{Y}_{\ell j\Omega}|V_{\rm coupl}|\mathbf{Y}_{\ell' j'\Omega}\rangle R_{\ell' j'\Omega}(r), \tag{8}$$

where

$$\langle \mathbf{Y}_{\ell j\Omega}|V_{\rm coupl}|\mathbf{Y}_{\ell' j'\Omega}\rangle$$
$$= -\beta\,k(r)\,\langle \mathbf{Y}_{\ell j\Omega}|Y_{20}(\hat{r})|\mathbf{Y}_{\ell' j'\Omega}\rangle$$
$$= -\beta\,k(r)\,(-1)^{\Omega-1/2}\sqrt{\frac{(2j+1)(2j'+1)}{20\pi}}$$
$$\times C(j, j', 2; \Omega, -\Omega, 0)\,C\left(j, j', 2; \frac{1}{2}, -\frac{1}{2}, 0\right). \tag{9}$$

The eigenvalue $\varepsilon_\Omega(<0)$ of the coupled equations (8) for a given value of Ω is obtained by integrating the equations in coordinate space for given values of β and radius R, with the asymptotic behavior of $R_{\ell j\Omega}(r)$ for $r \to \infty$

$$R_{\ell j\Omega} \propto r\,h_\ell(\alpha r), \tag{10}$$

where $h_\ell(-iz) \equiv j_\ell(z) + in_\ell(z)$, in which j_ℓ and n_ℓ are spherical Bessel and Neumann functions, respectively, and

$$\alpha^2 \equiv -\frac{2m\,\varepsilon_\Omega}{\hbar^2}. \tag{11}$$

The normalization condition is written as

$$\sum_{\ell,j}\int_0^\infty |R_{\ell j\Omega}(r)|^2\,dr = 1. \tag{12}$$

For spherical shape ($\beta = 0$) the eigenvalues depend only on (ℓ, j) and the Schrödinger equation is integrated in the laboratory coordinate system with the correct asymptotic behavior of wave functions with (ℓ, j) at $r \to \infty$. For axially symmetric quadrupole-deformed shape an infinite number of channels with (ℓ, j, Ω) are coupled for a given Ω. In practice, the number of coupled channels or the maximum value of (ℓ, j) pairs included for a given Ω is determined so that the resulting eigenvalues and wave functions do not change in a meaningful way by taking a larger number of coupled channels. The coupled differential equations obtained from the Schrödinger equation are integrated in coordinate space with the correct asymptotic behavior of radial wave functions in respective (ℓ, j) channels for $r \to \infty$. The solution obtained in this way is independent of the upper limit of radial integration, $R_{\rm max}$, if $f(r)$ in (4) and $k(r)$ in (5) are already negligible at $r = R_{\rm max} \gg R$. The r dependence of a given (ℓ, j) component thus obtained is generally different from that of any eigenfunctions in the spherically symmetric potential.

The Hamiltonian and how to solve the coupled differential equations derived from the Schrödinger equation for one-particle resonant levels in the deformed potential are described in Ref. [11]. Since one-particle resonant levels are not the main subject of the present article, for the details I just refer to Ref. [11], in which one-particle resonant energy $\varepsilon_\Omega{}^{\rm res}$ is sought so that eigenphase δ_Ω increases through $\pi/2$ as ε_Ω increases.

I take the diffuseness $a = 0.67$ fm and the radius $R = r_0A^{1/3}$ with $r_0 = 1.27$ fm, which are the standard parameters used in β stable nuclei [1]. The depth of the Woods-Saxon potential in (1) is

$$V_{WS} = -51 \pm 33\,\frac{N-Z}{A}\ \text{MeV}, \tag{13}$$

where the upper sign (+) is for neutrons while the lower one (−) is for protons. Since $A = N + Z$, the depth is a function of N/Z independent of the mass number A.

Though the shape of a nucleus is determined by both neutrons and protons, here I examine the dependence of shape on the shell structure of neutrons and protons, separately. In the discussion of the possible shape of a given nucleus I use the following empirical facts. First, from the shell structure in spherically symmetric potential, (a) the presence of a considerable energy gap in one-particle energy spectra for spherical shape indicates that spherical shape is preferred for the nucleon number, filling particles up to the levels below the gap. This fact is well known from the energy spectra for nuclei with magic numbers of nucleons. (b) The presence of some particles in a few almost degenerate (ℓ, j) shells around the Fermi level suggests that the nuclei may be deformed, as those particles have the possibility of gaining energy by breaking spherical symmetry (Jahn-Teller effect). This fact is known, for example, from the observation of deformed nuclei when both neutron and proton numbers are away from magic numbers by several particles. If pair correlation is not effective in some nuclei, it may be possible for nuclei with one or two nucleons in the almost degenerate (ℓ, j) shells to be deformed. This phenomena includes the case that one-particle levels of some almost degenerate (ℓ, j) shells lie in the continuum as one-particle resonant levels, if energies of the one-particle levels connected to the degenerate (ℓ, j) shells for spherical shape come down to be bound when the potential is deformed. A good example of this case is the deformation of ${}^{34}_{12}\mathrm{Mg}_{22}$, shown in Fig. 2 of Ref. [12]. Second, from the shell structure in axially symmetric quadrupole-deformed potential (c) the

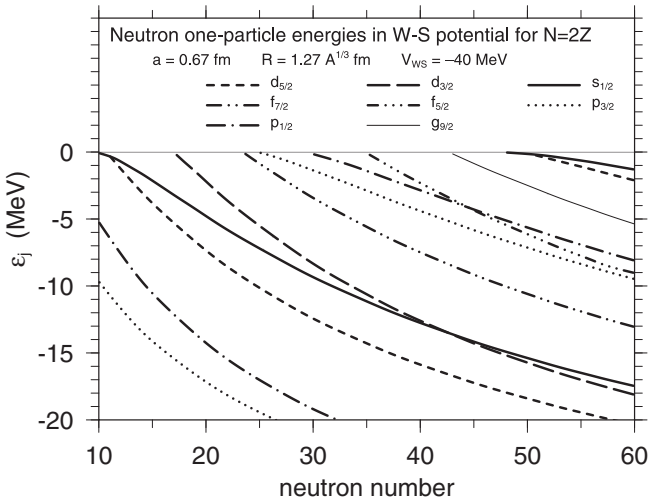

FIG. 1. Calculated neutron one-particle energies in a spherically symmetric Woods-Saxon potential produced by nuclei with $N/Z = 2$, which determines $V_{WS} = -40$ MeV. The ratio $N/Z = 2$ is an approximate ratio of the even-even core of the observed heaviest odd-N nuclei for a given even-Z in the lighter mass region. The Fermi levels of nuclei with respective neutron numbers lie around $\varepsilon_j = 0$.

presence of a considerable energy gap in one-particle energy spectra for a given deformation indicates that the configuration filling particles in the energy levels up to the levels below the gap is relatively stable for the nucleon number at the deformation. (d) The deformation at which some energy levels are almost degenerate may not be preferred by the nucleon number corresponding to partial filling of those energy levels, because those nucleons have the possibility of gaining energy by breaking the symmetry of axially symmetric quadrupole deformation (Jahn-Teller effect). (e) A very approximate measure of finding deformed nuclei is that the energies of most one-particle levels in the last filled major shell are going down as $|\beta|$ increases from zero. This measure is in good agreement with finding the prolately deformed region of stable rare-earth nuclei. See, for example, Fig. 5-3 of Ref. [5]. However, this approximate measure should not be used for very large deformations, at which various other factors such as surface tension, higher-order deformation, etc., may start to play an appreciable role.

III. NUMERICAL RESULTS

A. Light neutron drip line nuclei ($N/Z = 2$) with $10 < N < 60$

As is already written in the Introduction, an approximate ratio N/Z of the even-even core of the observed heaviest odd-N nuclei of $_6$C, $_8$O, $_{10}$Ne, and $_{12}$Mg isotopes is about 2. Thus, in order to see the systematic shell- structure of neutrons in neutron drip line nuclei, in Fig. 1 I show the neutron one-particle energies as a function of the neutron number, taking $N/Z = 2$. For $N/Z = 2$ the depth of the Woods-Saxon potential V_{WS} is -40 MeV. In Fig. 1 the Fermi levels of nuclei with respective N values lie around $\varepsilon_j = 0$. This can be seen by checking the Fermi level by filling N neutrons from the bottom, $1s_{1/2}$ level, though the $1s_{1/2}$ energy is outside the figure; for example, -33.1 MeV for $N = 60$ and -21.1 MeV for $N = 10$, respectively. For example, the one-particle level scheme for the $_{12}$Mg isotope is the one for the potential provided by $^{36}_{12}$Mg$_{24}$, while that for the $_{26}$Fe isotope is the one for the potential provided by $^{78}_{26}$Fe$_{52}$.

It is seen that in the spherical potential produced by $^{12}_{4}$Be$_8$ the energies of $2s_{1/2}$ and $1d_{5/2}$ levels are almost degenerate, in the spherical potential by $^{36}_{12}$Mg$_{24}$ the energies of $2p_{3/2}$ and $1f_{7/2}$ levels are almost degenerate, and in the potential produced by $^{78}_{26}$Fe$_{52}$ the energies of $3s_{1/2}$ and $2d_{5/2}$ levels are almost degenerate. The degeneracy of respective two levels in the spherical potential was expected for respective neutron drip line nuclei, and the possible resulting deformation and the related halo phenomena have been partly discussed in Refs. [2,12]. Nevertheless, it is useful to see them in this more systematic way, even if the neutron numbers of neutron drip line nuclei for respective isotopes may not strictly agree with experimental information. The prominent change of the neutron level structure in the spherical potential especially for $|\varepsilon_j| \lesssim 7$ MeV and the related physics are described in Fig. 2-30 and pp. 239–240 of Ref. [1]. A figure similar to a part of Fig. 1 is found in Ref. [13] in relation to the description of a new magic number $N = 16$.

One sees that the behavior of energy eigenvalues of weakly bound neutron orbits with smaller orbital angular momentum is different from that with larger orbital angular momentum, for example, by examining the energy variation of the $2s_{1/2}$ level relative to that of $1d$ levels as a function of N in Fig. 1. For the system with $N = 60$ the $2s_{1/2}$ level lies above both the $1d_{5/2}$ and $1d_{3/2}$ levels. In contrast, for the system with $N = 10$ the $2s_{1/2}$ level lies lower than both $1d$ levels. Though by going from $N = 60$ to $N = 10$ in Fig. 1 the depth of the Woods-Saxon potentials remains the same, the volume of the potential becomes smaller by about a factor of 6 since the mass number changes from 90 to 15. The energies of both $1d$ orbits change more or less smoothly from -20 to 0 MeV. In contrast, the energy curve of the $2s_{1/2}$ orbit changes strongly, in particular for $|\varepsilon_j| \lesssim 3$ MeV. This is because since there is no centrifugal barrier for s orbits, the probability for s neutrons to remain inside the potential is zero in the limit that eigenenergies $\varepsilon_{s1/2}$ (<0) approach zero. Namely, weakly bound neutrons in the s orbit spend most of the time outside the potential produced by core nuclei as the one-particle energy $\varepsilon_j < 0$ approaches zero. The slope of the curve of $s_{1/2}$ orbits in Fig. 1, $d\varepsilon_j/dN$, approaches zero in the limit of $\varepsilon_j(<0) \to 0$. In contrast, neutrons in the d orbits lose the binding energy relatively more rapidly as the binding field becomes weaker, because due to the presence of the centrifugal barrier the major part of the wave function stays inside the potential [1,2,4]. The same physics coming from the considerable difference between the heights of centrifugal barriers produces the phenomena in Fig. 1 that the $2p_{3/2}$ energy approaches the $1f_{7/2}$ energy as the one-particle binding energies approach zero.

B. Neutron-rich nuclei ($N/Z = 1.7$) with $40 < N < 90$

A basic question is whether or not the shell structure in neutron-rich nuclei around the r process is approximately the same as that of stable nuclei if the shell structure around

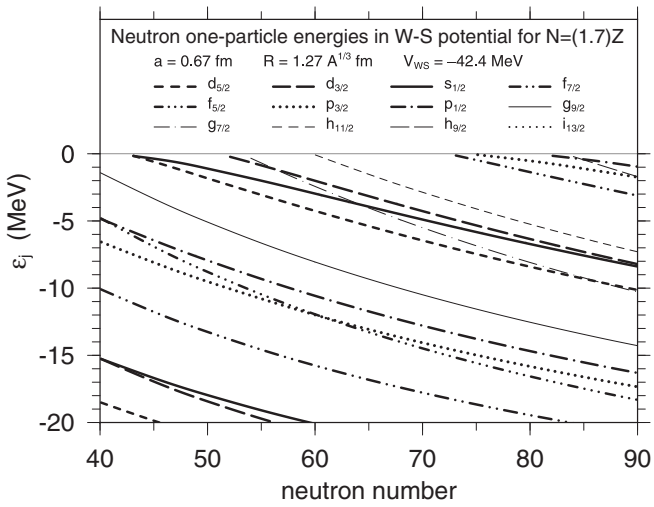

FIG. 2. Calculated neutron one-particle energies in a spherically symmetric Woods-Saxon potential produced by nuclei with $N/Z = 1.7$, which determines $V_{WS} = -42.4$ MeV. The ratio $N/Z = 1.7$ is an approximate ratio in lighter nuclei related to the r process just above $^{78}_{28}\mathrm{Ni}_{50}$. The Fermi levels of nuclei with respective neutron numbers lie around $\varepsilon_j = -4$ MeV.

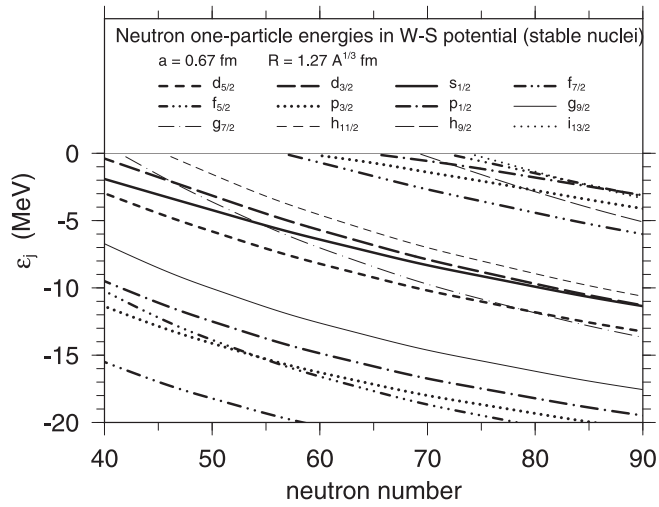

FIG. 3. Calculated neutron one-particle energies in a spherically symmetric Woods-Saxon potential produced by nuclei along the stability line. The depth of the Woods-Saxon potential is determined by the formula (13) using the proton number given by respective neutron numbers along the stability line. Thus, the depth of the potential changes as a function of neutron number. The Fermi levels of nuclei with respective neutron numbers lie around $\varepsilon_j = -8$ MeV.

the same neutron number is examined in the two cases. The shell structure around respective Fermi levels is, in practice, of interest. I examine the question by using the present phenomenological one-body potential, since the study of the shape and shell- structure by using the present potential has been successful at least in light neutron drip line nuclei.

In Fig. 2 the neutron one-particle energy eigenvalues as a function of neutron number are shown, taking $N/Z = 1.7$, which determines the depth of the potential to be $V_{WS} = -42.4$ MeV. The N/Z ratio is an approximate ratio in lighter nuclei related to the r process just above $^{78}_{28}\mathrm{Ni}_{50}$. The ratio $N/Z = 1.7$ in this mass region means that the neutron excess corresponds roughly to one major shell in the sense of the traditional shell model. The Fermi levels of relevant nuclei in Fig. 2 lie around $\varepsilon_j \approx -4$ MeV. For example, the one-particle energy spectrum at $N = 68$ in Fig. 2 is the one produced by the potential of $^{108}_{40}\mathrm{Zr}_{68}$.

For comparison, in Fig. 3 the neutron one-particle energy eigenvalues of the potential produced by nuclei along the stability line are shown as a function of neutron number. The Fermi levels of relevant nuclei lie around $\varepsilon_j \approx -8$ MeV. Roughly speaking, deformation is not particularly favored by the proton numbers of nuclei corresponding to the neutron numbers in Fig. 3, in contrast to the fact that deformation may be favored by the proton numbers of nuclei in the region of $60 \lesssim N \lesssim 70$ of Fig. 2. This is because, for example, in the region of $50 \lesssim N \lesssim 70$ of stable nuclei, protons gradually fill in the single high-j ($1g_{9/2}$) shell. The comparison of eigenvalues in Fig. 3 with observed low-lying spectra of relatively simple spherical nuclei seems good. For example, the observed spin-parities of the ground, first excited, and second excited states of $^{121}_{50}\mathrm{Sn}_{71}$ are $3/2+$, $11/2^-$, and $1/2^+$, respectively, which should be compared with ε_j values at $N = 70$ in Fig. 3. Another example is that the observed spin-parities of the ground and first excited states of $^{91}_{40}\mathrm{Zr}_{51}$ are $5/2^+$ and $1/2^+$, respectively, which should be compared with ε_j values at $N = 50$ in Fig. 3.

A very systematic behavior of ε_j which is found in Figs. 1, 2, and 3 is that, as a function of neutron number, ε_j (<0) of lower-ℓ orbits decreases more slowly than ε_j of higher-ℓ orbits. In contrast, in the harmonic oscillator (HO) potential without a spin-orbit potential the levels of the $2s$ and $1d$ neutrons are degenerate. The higher energy of the $2s$ level than the $1d$ levels at $N = 60$ seen in Fig. 1 is explained by considering the difference of the radial shape of the Woods-Saxon potential from that of the HO potential (see p. 222 of Ref. [1]). On the other hand, in order to find the effect of the presence of nuclear surface together with the quantum-mechanical leaking of bound one-particle wave functions to the outside of the surface on the eigenvalues ε_j, I pay attention to the eigenvalues of neutrons in the infinite square-well potential (cavity) without spin-orbit potential. In the cavity there is no leaking of wave functions to the outside of the potential. The eigenvalues $\varepsilon_{n\ell}$ are obtained from the nth zero of the spherical Bessel function of order ℓ. Then, among the family with $\Delta\ell = 2$ originating from a given HO major shell the one-particle energies decrease as ℓ increases [6]. For example, the $(n+1)s$ level is energetically always higher than the nd level. This simple example shows an important role of the nuclear surface in the shell structure of one-particle energies in finite potentials.

When the shell structure for a given N around the Fermi level in Fig. 2 is compared with that in Fig. 3, the main systematic difference comes from the fact that the decrease of ε_j of low-j orbits is more moderate than that of high-j orbits as neutron number increases. A typical example is that for $N = 65$ in Fig. 2 the $1g_{7/2}$ level is nearly degenerate

to the $3s_{1/2}$ level at $\varepsilon_j \approx -4$ MeV, while for $N = 65$ in Fig. 3 the former is lower than the latter by more than 1 MeV around $\varepsilon_j = -8$ MeV. This difference comes mainly from the difference of the Fermi energies in Figs. 2 and 3. As the neutron number decreases (namely, as the potential gets weaker), the binding energies of all j orbits smoothly decrease; however, the higher-ℓ orbits decrease the binding energies appreciably more than the lower-ℓ orbits. This kind of shell-structure change within a given one major shell is systematically present in finite-well potentials, as described in the previous paragraphs, though there can be, in practice, other locally stronger shell-structure changes in neutron one-particle spectra, which come, for example, from a strong attractive neutron-proton interaction depending on the proton orbits occupied. The systematic change of shell structure can have a serious effect, for example, on the spin-parities of respective low-lying states and the related observed quantities, while the effect on some other observed quantities may be to some extent smoothed out when the system has a finite temperature, as in the r process.

C. Cr or Fe isotopes with $N/Z \approx 1.7$

I focus on the shell structure in the potential provided by ${}^{66}_{24}\mathrm{Cr}_{42}$ and ${}^{70}_{26}\mathrm{Fe}_{44}$, for which the ratio N/Z is equal to 1.75 and 1.69, respectively. Since the calculated shell-structure of these two nuclei is very similar, in the following the numerical result of only ^{70}Fe is presented. The recent experimental information [7,8] indicates that even-even Cr isotopes with $N = 38$–42 and even-even Fe isotopes with $N = 40$–46 are deformed, based on both the observed very low energies of the first excited state, which is assumed to be 2^+ in some cases, and the observed ratios of $E(4_1^+)/E(2_1^+)$, where the second excited state is assumed to be 4^+ in some cases. An interesting question is whether or not Cr isotopes with $N > 42$ and Fe isotopes with $N > 46$ are also deformed. The question is related to the basic origin of the deformation in terms of neutron shell structure, as the neutrons with $N > 40$ are expected to occupy the single j shell, $1g_{9/2}$, in the simple picture of spherical shape.

In Fig. 4 the calculated proton one-particle energies in the potential produced by ^{70}Fe as a function of deformation β are shown, while the calculated neutron one-particle energies in the potential provided by ^{70}Fe are exhibited in Fig. 5. It is seen from Fig. 4 that some moderate-size prolate deformation may be favored by proton numbers $Z = 24$ (Cr) and 26 (Fe) while some oblate deformation may be certainly disfavored. The preference of prolate deformation is consistent also with the recent experimental finding in Ref. [14] of the rotational spectra based on the $5/2^-$ ground state in ${}^{65,67}_{25}\mathrm{Mn}_{40,42}$. In Fig. 4 it is also noted that the proton one-particle energy difference between the $2d_{5/2}$ and $1g_{9/2}$ levels is as large as 5.37 MeV, while the energy difference between the $1g_{9/2}$ and and $2p_{1/2}$ levels is only 1.57 MeV. In short, $Z = 50$ is a good magic number, as in stable nuclei.

From Fig. 5 it is seen that the neuron one-particle energy difference between the $2d_{5/2}$ and $1g_{9/2}$ levels is 2.62 MeV, while the one between the $1g_{9/2}$ and $2p_{1/2}$ levels is 3.15 MeV. Namely, for spherical shape the $N = 50$ energy gap is smaller

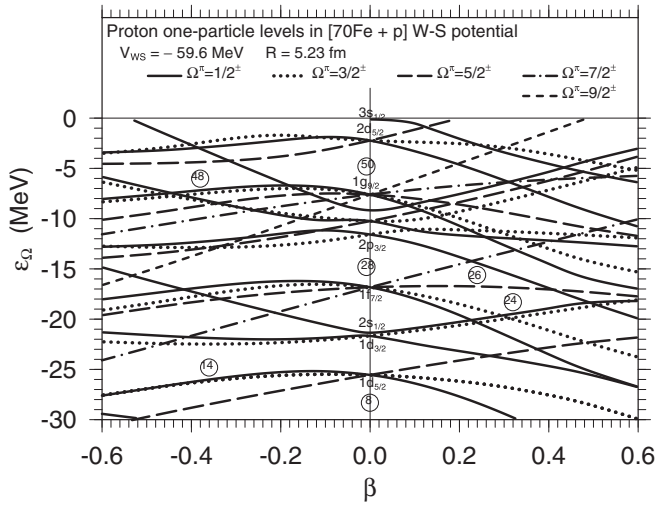

FIG. 4. Calculated proton one-particle energies in the potential produced by ^{70}Fe as a function of quadrupole deformation β. Some proton numbers, which are obtained by filling all lower-lying levels, are indicated with open circles. For spherical shape ($\beta = 0$) the quantum numbers $(n\ell_j)$ of orbits are denoted except for $2p_{1/2}$ at $\varepsilon_j = -9.16$ MeV and $1f_{5/2}$ at $\varepsilon_j = -10.24$ MeV.

than the $N = 40$ energy gap. Since the one-particle levels above $N = 50$ such as the $2d_{5/2}$ and $3s_{1/2}$ levels have the same positive parity as $1g_{9/2}$, there is a possibility of being mixed with $1g_{9/2}$ by the quadrupole-deformed field so as to lower the energies of lowest-lying levels with given Ω values, which are the levels connected to the $1g_{9/2}$ state at $\beta = 0$. The

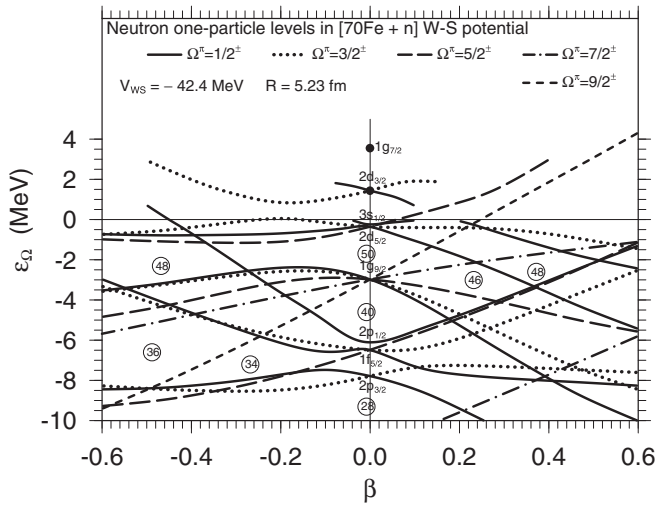

FIG. 5. Calculated neutron one-particle energies in the potential produced by ^{70}Fe as a function of quadrupole deformation β. Some neutron numbers, which are obtained by filling all lower-lying levels, are indicated with open circles. One-particle bound and resonant energies at $\beta = 0$ are -7.80, -6.52, -6.14, -2.99, -0.37, -0.25, $+1.44$, and $+3.56$ MeV for the $2p_{3/2}$, $1f_{5/2}$, $2p_{1/2}$, $1g_{9/2}$, $2d_{5/2}$, $3s_{1/2}$, $2d_{3/2}$, and $1g_{7/2}$ levels, respectively. One-particle resonant levels ($\varepsilon_\Omega > 0$) for $\beta \neq 0$ are not plotted if they are not relevant to the present interest.

appreciable amount of such mixture in the $\Omega^\pi = 1/2^+, 3/2^+$, and $5/2^+$ orbits can be seen from the dependence of those one-particle energies on β in Fig. 5. Due to the relatively large energy distance between the neutron $1g_{9/2}$ and $2p_{1/2}$ levels and the strong quadrupole coupling between the $1g_{9/2}$ and $2d_{5/2}$ orbits, the possibility of lowering the energy of the system in the region of $N \lesssim 46$ is seen by filling one-particle levels for the moderate-size prolate deformation. In short, examining the behavior of one-particle energies for prolate deformation $\beta \approx 0.2$, one may expect that both Cr and Fe isotopes can be prolately deformed up to $N \approx 46$.

Experimental information on the spin-parity of the ground state of neutron-rich ($N > 40$) odd-N Fe isotopes is not yet sufficiently established. However, some experimentally suggested spin-parities, $5/2^+$ for $^{67}_{26}\mathrm{Fe}_{41}$ [15] and $1/2^-$ for $^{69}_{26}\mathrm{Fe}_{43}$ [16], are difficult to obtain for spherical shape. In contrast, as is seen in Fig. 5 it is pretty easy to expect those spin-parities if those nuclei are prolately deformed by a moderate amount. This expectation is valid also in the case that a proper pair correlation is included in the consideration.

I compare the shell structure of neutron-rich nuclei in the present $N = 40$ region with that of the $N = 20$ IoI region. The similarities of the neutron shell structure for spherical shape of neutron-rich nuclei in the two regions are (a) the lower one-particle shells are high-j shells, $1f_{7/2}$ and $1g_{9/2}$, which are energetically pushed down from respective major shells by the large ℓ-s splitting in the sense of Ref. [17]; (b) the higher one-particle shells, $2p_{3/2}$ and $2d_{5/2}$, are weakly bound (or resonant) and have smaller orbital angular momenta than the respective lower ones by $\Delta\ell = 2$. Thus, the energy distance between the higher and lower shells becomes smaller compared with that in deeply bound cases [2]. Furthermore, the higher shells can be strongly quadrupole coupled with respective lower ones due to $\Delta\ell = 2$ and $\Delta j = 2$. On the other hand, the differences are (c) due to the smaller ℓ-s splitting in the f shell than in the g shell the lowering of the $1f_{7/2}$ level is smaller than that of the $1g_{9/2}$ level; (d) for a given small binding energy the degree of energy lowering of the $2p_{3/2}$ ($\ell = 1$) level due to the leaking of the wave function to the outside of the surface is larger than that of the $2d_{5/2}$ ($\ell = 2$) level.

As an example of the neutron potential provided by deformed nuclei in the $N = 20$ IoI region I take the potential given by $^{34}_{12}\mathrm{Mg}_{22}$ (where $N/Z = 1.83$), which is shown in Fig. 2 of Ref. [12]. For spherical shape ($\beta = 0$) the large energy gap (4.51 MeV) at $N = 20$ is kept well, while the energy difference between the $2p_{3/2}$ and $1f_{7/2}$ is only 0.391 MeV. Namely, the $2p_{3/2}$ and $1f_{7/2}$ levels are almost degenerate and the spherical energy gap at $N = 28$ or the magic number $N = 28$ has totally disappeared. Consequently, neutrons in those neutron-rich Mg isotopes partially filling the combined $(2p_{3/2} + 1f_{7/2})$ shell may easily make the energy of the system lower by causing deformation. A simple approximate way often used to guess possible deformation using figures such as Fig. 2 of Ref. [12] is to examine the deformation dependence of the energy of the last-filled (Fermi) one-particle level for a given N. I note that, for example, in the degenerate harmonic-oscillator model the first (second) half of a given major shell has prolate (oblate) shape, and the slope of one-particle energy as a function of prolate deformation changes from downward to upward just in the middle of the major shell. Considering only prolate shape, the Fermi energy of the deformed system with $20 \leqslant N \leqslant 28$ can become lower than that of spherical shape, which is equal to $\varepsilon(1d_{3/2})$ for $N = 20$ and $\varepsilon(1f_{7/2})$ for $21 \leqslant N \leqslant 28$. Since the $(2p_{3/2} + 1f_{7/2})$ shell accommodates 12 neutrons, the isotopes with up to 6–8 neutrons in the combined shell could be expected to be prolately deformed [2], neglecting pair correlation in these light nuclei. Later this expectation was experimentally found to be fulfilled [18]. In contrast, at $\beta = 0$ in Fig. 5 the energy gap (2.62 MeV) at $N = 50$ is small but it is not close to zero. This appreciable energy gap leads to the fact that the Fermi energy of the $N = 50$ system within moderate prolate deformation in Fig. 5 never becomes lower than that of spherical shape, which is equal to $\varepsilon(1g_{9/2})$. If the $2d_{5/2}$ and $1g_{9/2}$ shells had been nearly degenerate, for $\beta > 0$ all downward-going levels originating from the two shells would have been gathered in the energetically lower half as in the case of the level structure coming from the combined $(2p_{3/2} + 1f_{7/2})$ shell seen in Fig. 2 of Ref. [12]. Then, deformed shape might have been preferred for up to 10 neutrons in the combined $(2d_{5/2} + 1g_{9/2})$ shell, which is slightly more than a half of the neutron number that can be accommodated in the combined $(2d_{5/2} + 1g_{9/2})$ shell. Namely, deformed shape might have been possible continuously up to $N = 50$. However, in the present case it is expected that the Fe and Cr isotopes only up to $N \approx 46$ may be prolately deformed by an appreciable amount.

The characteristic features of the calculated neutron one-particle energies in the potential provided by $^{76}_{26}\mathrm{Fe}_{50}$ are very similar to those of Fig. 5. For example, the depth of the potential is -40.6 MeV and one-particle energies at $\beta = 0$ are -3.11, -0.47, and -0.29 MeV for the $1g_{9/2}$, $2d_{5/2}$, and $3s_{1/2}$ levels, respectively. Namely, the energy distance between the $2d_{5/2}$ and $1g_{9/2}$ levels is 2.64 MeV. In Ref. [8] it was wondered whether or not the deformation extends to $N = 50$ in the $_{24}$Cr and $_{26}$Fe isotopes, though in Ref. [8] no results of shell-model calculations were given for those isotopes, for which experimental data have not been obtained. In my present work I conclude that the deformation continuing up to $N = 50$ is unlikely.

IV. CONCLUSION AND DISCUSSIONS

In the present work I have studied the shape and shell structure of lighter neutron-rich nuclei away from the stability line, by using the Woods-Saxon potential, for which parameters are phenomenologically determined so as to reproduce the properties of neutron-rich stable nuclei. The success and usefulness of the Woods-Saxon potential have been already known in the study of the properties related to one-particle operators in light neutron drip line nuclei.

First, I showed calculated neutron one-particle energies in lighter neutron drip line nuclei taking the ratio $N/Z = 2$ and the region $10 \leqslant N \leqslant 60$. From Fig. 1 one sees the approximate neutron number at which spherical (or deformed) halo phenomena are expected to occur, and the reason why the halo may be observed. The deformed halos around $N \approx 10$

(for example, $^{11}_{4}\mathrm{Be}_{7}$) due to the almost degeneracy of the $2s_{1/2}$ and $1d_{5/2}$ levels and around $N \approx 24$ (for example, $^{37}_{12}\mathrm{Mg}_{25}$) due to the almost degeneracy of the $2p_{3/2}$ and $1f_{7/2}$ levels are already experimentally confirmed. Therefore, one may expect another spherical or deformed halo around $N = 51$ (for example, $^{77}_{26}\mathrm{Fe}_{51}$). It is interesting to see in Fig. 1 that deformation may play a role almost whenever halo phenomena (with s or p components of neutrons) are expected. I note that, due to the simplicity of the present one-body potential, one can easily obtain a systematic view of the shell structure around the neutron drip line, compared with sophisticated and elaborated microscopic models starting with effective two-body interactions.

Second, I studied the neutron shell structure of lighter neutron-rich nuclei related to the r process just above $^{78}_{28}\mathrm{Ni}_{50}$, choosing $N/Z = 1.7$ and $40 \leqslant N \leqslant 90$. If the proton numbers accept deformation, some even-even nuclei in the region of $60 \lesssim N \lesssim 70$ in Fig. 2 may be prolately deformed among the nuclei in the major shell $50 \leqslant N \leqslant 82$, following the mechanism similar to the case in which the stable rare-earth nuclei with $90 \lesssim N \lesssim 112$ are deformed among the nuclei in the major shell $82 \leqslant N \leqslant 126$. The spherical shell structure around the Fermi level ($\varepsilon_j \approx -4$ MeV) for a given neutron number is compared with the shell structure of stable nuclei around the Fermi level ($\varepsilon_j \approx -8$ MeV) for the same neutron number. Since the shell structure around the Fermi level of stable nuclei is well studied, one may use the idea that information known in stable nuclei can be used in the analysis of r-process nuclei, when the neutron number is the same in the two cases. Taking the same neutron number around respective Fermi levels, the main difference of the shell structure of the r-process nuclei in this mass number region from that of stable nuclei is found to come essentially from the difference between the Fermi energies, $\varepsilon_j \approx -4$ MeV versus $\varepsilon_j \approx -8$ MeV. Namely, as the neutron number decreases (i.e., the potential becomes weaker), higher-ℓ orbits lose the binding energies more rapidly than lower-ℓ orbits. That means, within a given major shell, the binding energies of higher-ℓ orbits around the Fermi energy of stable nuclei are larger than those of lower-ℓ orbits by an order of 1 MeV compared with the case around the Fermi energy of the r-process nuclei. Though the order of 1 MeV is an appreciable change of the shell structure within a given major shell, due to the possible deformation in nuclei of Fig. 2 and the finite temperature present in the r-process nuclei it is not trivial how much effect this kind of basic shell-structure difference in r-process nuclei from that in stable nuclei has on some observed quantities, before calculations of some individual nuclei are quantitatively examined.

Third, I presented the study of the shell structure for the potential provided by $^{70}_{26}\mathrm{Fe}_{44}$ ($N/Z = 1.69$), which is a representative example of so-called N=40 IoI nuclei. It is experimentally indicated that even-even Cr isotopes with $N = 38$–42 and even-even Fe isotopes with $N = 40$–46 are deformed. In the present model the possible deformation of Fe isotopes with $40 < N \lesssim 46$ is expected, while deformation of the nucleus $^{66}_{26}\mathrm{Fe}_{40}$ is not obtained because the Fermi level of the $N = 40$ system in the region of moderately deformed prolate shape never becomes lower than that of spherical shape, which is equal to $\varepsilon(2p_{1/2})$. In this respect I note that though the observed $\mathrm{E}(2^+_1) = 574$ keV in ^{66}Fe is pretty small and may indicate deformation, the observed ratio of $E(4^+_1)/E(2^+_1)$ is only 2.45. The very small ratio compared with 3.33 indicates that ^{66}Fe is not a stably deformed nucleus.

Though in the literature it is wondered whether or not the $N = 40$ IoI deformation extends to $N = 50$ in the $_{24}$Cr and $_{26}$Fe isotopes, from Fig. 5 I conclude that the Fe and Cr isotopes may be prolately deformed only up to $N \approx 46$, and that the deformation continuing up to $N = 50$ is unlikely, because of a few MeV energy difference between the $2d_{5/2}$ and $1g_{9/2}$ orbits at $\beta = 0$ in "$N = 40$ IoI" nuclei in contrast to the almost degenerate $2p_{3/2}$ and $1f_{7/2}$ orbits at $\beta = 0$ in "$N = 20$ IoI" nuclei. The consequence of this difference on the possible deformation in relevant nuclei is explained in detail in Sec. III C.

In the present work I have concentrated on the discussion of the fundamental shell structure of one-particle energy spectra and did not take into account the role of pair correlation. The shell structure which I have discussed is anyway the first important quantity before including pair correlation. In the quantitative comparison with experimental data the inclusion of pair correlation may be necessary, perhaps except for light halo nuclei such as those discussed in Sec. III A. In some r-process nuclei discussed in Sec. III B nonzero temperature together with deformation and pair correlation is further necessary to be included in the quantitative comparison with experimental information. In the region of "$N = 20$ IoI" nuclei (for example, neutron-rich Mg isotopes) a model in line with the present article could well explain available experimental data. Since the shell structure in the region of "$N = 40$ IoI" is, in some part, similar to that in the region of "$N = 20$ IoI" as discussed in Sec. III C, it will be interesting to see how far the result presented in Sec. III C is in agreement with findings in experiments in the future.

[1] A. Bohr and B. R. Mottelson, *Nuclear Structure*, Vol. I (Benjamin, Reading, MA, 1969).
[2] I. Hamamoto, Phys. Rev. C **76**, 054319 (2007).
[3] I. Hamamoto, Phys. Rev. C **81**, 021304(R) (2010).
[4] I. Hamamoto, Phys. Scr. **91**, 023004 (2016).
[5] A. Bohr and B. R. Mottelson, *Nuclear Structure*, Vol. II (Benjamin, Reading, MA, 1975).
[6] I. Hamamoto and B. R. Mottelson, Phys. Rev. C **79**, 034317 (2009).
[7] G. Benzoni *et al.*, Phys. Lett. B **751**, 107 (2015).
[8] C. Santamaria *et al.*, Phys. Rev. Lett. **115**, 192501 (2015).
[9] A. Gade and B. M. Sherrill, Phys. Scr. **91**, 053003 (2016).
[10] I. Hamamoto, Phys. Rev. C **69**, 041306(R) (2004).
[11] I. Hamamoto, Phys. Rev. C **72**, 024301 (2005).
[12] I. Hamamoto, Phys. Rev. C **85**, 064329 (2012).
[13] A. Ozawa, T. Kobayashi, T. Suzuki, K. Yoshida, and I. Tanihata, Phys. Rev. Lett. **84**, 5493 (2000).

[14] X. Y. Liu *et al.*, Phys. Lett. B **784**, 392 (2018).
[15] H. Junde, H. Xiaolong, and J. K. Tuli, Nucl. Data Sheets **106**, 159 (2005).
[16] C. D. Nesaraja, Nucl. Data Sheets **115**, 1 (2014).
[17] M. G. Mayer, Phys. Rev. **75**, 1969 (1949); O. Haxel, J. H. D. Jensen, and H. E. Suess, *ibid.* **75**, 1766 (1949).
[18] P. Doornenbal, H. Scheit, S. Takeuchi, N. Aoi, K. Li, M. Matsushita, D. Steppenbeck, H. Wang, H. Baba, H. Crawford, C. R. Hoffman, R. Hughes, E. Ideguchi, N. Kobayashi, Y. Kondo, J. Lee, S. Michimasa, T. Motobayashi, H. Sakurai, M. Takechi, Y. Togano, R. Winkler, and K. Yoneda, Phys. Rev. Lett. **111**, 212502 (2013).